

REVIEW ARTICLE

Advances in Graphene-based Materials for Dye-sensitized Solar Cell Components, Electronic Devices and Prospective Applications: A Critical Review

Azeez Surajudeen O¹, Surajudeen Sikiru^{2,6*}, Oladosu Temidayo Lekan³, Yekinni Kolawole Sanusi^{4,6}, Akeem Adekunle Adewale¹ and Abiodun Ayodele O.J⁵

¹Kwara State University, Malete, College of Pure and Applied Science, Department of Physics; ²Department of Fundamental and Applied Sciences, Universiti Teknologi, PETRONAS, Malaysia; ³Mechanical Engineering Department, Universiti Teknologi PETRONAS, Perak, Malaysia; ⁴Department of Pure and Applied Physics, Ladoke Akintola University of Technology, Nigeria; ⁵Department of Physical Science, Lead City University, Ibadan Oyo state; ⁶Noverlty Polytechnic Kisi Oyo State Nigeria

ARTICLE HISTORY

Received: December 16, 2020
Revised: April 27, 2021
Accepted: May 15, 2021

DOI:
10.2174/1573413717666210702095201

Abstract: The investigation of a dye-sensitized solar cell (DSSC) as an alternative approach to the conventional photovoltaic cell (silicon-based) is attracting remarkable attention recently. This stems from the excellent optical properties of graphene, such as impressive transparency, conductance in near-infrared and visible light spectrums, along with its thermochemical stability, as reported in the literature. However, the main limitation of graphene production is the lack of suitable methods for its industrial-scale synthesis. Consequently, the research on industrial applications of graphene development and understanding of how to **pragmatize** existing theoretical approaches are still ongoing in the related research domain. This is exemplified in single, few, and adhesive layer mechanical cleavage graphene methods, which are not yet practicable, as these methods will restrict the chance for scaling up. These limitations and inadequate reviews on graphene development impelled the authors to compile the advances in graphene synthesis, properties, recent applications, and future directions. The mechanical exfoliation synthesis technique delivers quality graphene films sized from 5 to 10 μm . Graphene-TiO₂ hybridization was also found to possess efficiency acclivity as high as 39%. This review provides significant implications for a better understanding of graphene performance indicators and insight for future research in photovoltaic or optical modulation devices.

Keywords: Dye-Sensitized Solar Cell, Graphene, TiO₂ hybridization, Optical properties.

1. INTRODUCTION

New approaches to create, store, and efficiently make use of solar energy have been studied for decades for producing reliable solar energy. Sun is a safe, cheap, and clean source of energy that can be directly converted to electricity without causing environmental problems. The conversion of sunlight to electricity through the photoelectric effect is achieved by using photovoltaic materials and devices [1, 2]. Carbon is a common material that has been ever found, whereas graphene is an allotropy of carbon with a single layer of atoms arranged in two-dimensional honeycomb lattices. Graphene is a single-layer sheet of sp² hybridized carbon atoms and has drawn much attention and research motives because of its modifiable properties [3]. In 1962, Hanns-Peter Boehm was the first to describe graphene structure as an allotrope of carbon; the matrix structure was examined by X-ray diffrac-

tion while studying various atoms of graphene particles [4, 5]. It is important to know that graphene consists of a single layer of carbon atoms forming the honeycomb structure; bounded together in a channel of reoccurrence hexagons in the plane of an atom; the bonds between the carbon atoms **are** about 0.0142 nm [6-9].

Graphene is a nanoparticle material with a large specific surface area of $2630 \text{ M}^2 \text{ g}^{-1}$, intrinsic mobility of $200,000 \text{ cm}^2 \text{ V}^{-1} \text{ S}^{-1}$ [10], Young's Modulus of $\approx 1.0 \text{ TPa}$, the thermal conductivity of $\approx 5000 \text{ W m}^{-1} \text{ K}^{-1}$ [11-13] and optical transmittance of 97.7%. In addition to the highlighted properties, graphene also exhibits a high electrical conducting ability, as well as the ability to withstand a current density of 108 A/cm^2 [13, 14]. These properties are contributory factors that make it suitable as a transparent conductive electrode (TCEs), which is a very important component in photovoltaic and display technology [15, 16]. It is pertinent to note that graphene is closely transparent with the

*Address correspondence to this author at the Department of Fundamental and Applied Sciences, Universiti Teknologi, PETRONAS, Malaysia; E-mail: surajudeen86@gmail.com

highest electrical conductivity and ambient temperature among engineering materials ever discovered [6, 17-22].

Graphene is a prospective material that is very useful in various fields of study because of the presence of high electron mobility, optical properties, thermal, chemical and tendency of high mechanical stability [23]. The major purpose of introducing graphene into the DSSC structure is to ameliorate electron conversion efficiency with better stability. It also implies that graphene acts as an electron transport layer in order to improve the transfer of electrons in the DSSC [24]. The perpetrated measurement of DSSC indicated that the addition of little graphene could increase the short circuit current and power conversion efficiency [25].

To date, quite a number of studies have investigated the application of graphene as transparent electrodes [26, 27] and ultrahigh-speed transistors [28]. In 2008, Xu et al. [29] also investigated soluble graphene-based electrocatalytic layer capable of remodeling the fluorine-doped tin oxide (FTO); the outcome of the work revealed graphene significance in the performance enhancement of the electrodes. Electrocatalytic activity of iodide graphene was also reported two years after by Hasin et al. [1]. Similarly, Roy-Mayhew et al. [10] explained that graphene sheets possess catalytic, electrical properties, and flexibility to serve as alternative electrodes. The result of the study revealed that the performance of the investigated dye-sensitized solar cells (DSSCs) was due to the C/O ratio of graphene and was reduced by a thermal process. Kavan et al. [11] reported that the physical and chemical properties of the graphene nano-platelets involved in the reduction and oxidation reaction are related to the concentration of defects and oxygen-containing groups. As being deduced in the literature, a defect in graphene has a substantive effect on the graphene performance as electrodes because of the improved active sites and hydrophilicity of the oxygen group. Nonetheless, the electrical conductivity of graphene may be reduced due to the electronics structure despite the high concentration of defects [30, 31].

Notwithstanding these promising properties of graphene, some graphene synthesis methods are yet to be pragmatic. The single, few, and adhesive layer mechanical cleavage graphene methods are not yet pragmatic, as these methods will restrict the chance for scaling up [32, 33] to synthesize a large number of graphene films on different substrates with methods agreeable with recent industrial technology; this approach will be important for future applications. Most discoveries in graphene technology are still under research; the question is, will the graphene revolution be limited to theoretical findings? The industrial applications are still very little, regardless of their attractive tensile strength and conductivity [34-36].

Although there are a few reviews on graphene in the public domain, the advances in graphene synthesis, properties, recent applications, and future directions are required to maximize the inherent potential of graphene among smart materials in the fifth-generation manufacturing era. Therefore, this review seeks to present the state of knowledge based on graphene synthesis, properties, current applications and future potentials. This compilation will inform relevant industries on graphene's inherent potentials and the means of

its optimization to fully compete with carbon nanotube and counterpart.

2. STRUCTURE AND PROPERTIES OF GRAPHENE

Graphene layers contribute to their electrocatalytic properties. Fig.1 presents the fundamental element of graphene's structures to ameliorate the understanding of its properties. For instance, the thermal conductive properties of pure graphene are traceable to the embedded structural holes that allow phonons transmittance when exposed to sunlight. However, because of structural band modification in graphene oxide and its hybrids, a better understanding of the effect of the structural holes phenomenon of graphene oxides with respect to their thermal properties has to be developed [37-39].

Although graphene is fundamentally categorized in the literature as metallic, metalloids, and non-metallic graphene [40], there is still no universal consensus regarding the elements that are responsible for graphene classification; some researchers consider metallic graphene with very low band gaps as a metalloid, which is backed up with some theories [39]. Through the acclivity in graphene studies, regular features of metallic, metalloids, and non-metallic materials have been observed to be remarkable. The photo responsiveness capability of graphene affirms its suitability for many latest technological applications [39]. The electrically conductive properties of graphene are quite impressive, and this will be cardinal for future generation systems or process designs. Also, massless relativistic behavior of some graphene due to the absence of band gap engenders valency-conduction superimposition [38, 41, 42].

The properties of graphene are reported in the literature to be influenced by the number of layers, defects, and their compositions. As it was opined that graphene possesses a higher surface area than its counterparts, carbon black and carbon-nano tube, which are about 2630, 850-900 m^2/g , and 100-1000 m^2/g , respectively [38, 42]. Few layered graphene, graphene oxide, and other derivatives are found to exhibit fewer surface areas than single-layer graphene [38, 42]. Fig. 2 indicates inter-atomic force, bandgap, and crystal structure that exist in graphene structure. The atomic forces in graphene structure are shown in Fig. 2a, which reveals a relative height of $4^0 A$ (a single layer) for a folded segment. Fig. 2b and 2c present a graphene sheet that relies on a micrometer-sized metallic scaffold and a very large graphene crystal, respectively. The blue and red lines in Fig. 2c show that the crystal's faces are zigzag and armchair edgeds, respectively.

3. GRAPHENE SYNTHESIS

Graphene was first discovered by the most prominent method of the micromechanical cleavage of graphite in order to synthesize high-quality defect-free graphene, and this process is also called "scotch tape", a method of peel off [35]. Chemical vapour deposition (CVD) was used as a workable alternative process after some time [43, 44]. More so, it was realized that these procedures offer a low production yield,

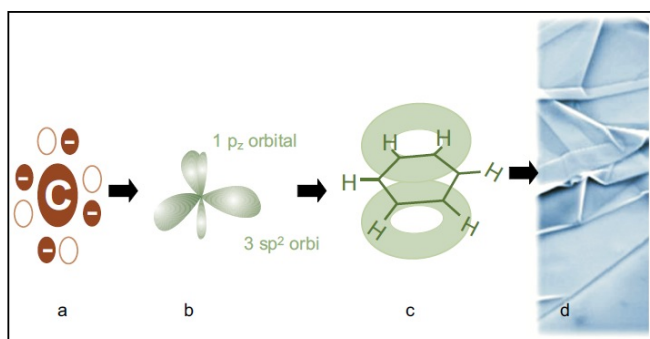


Fig. (1). (a-c) Graphene interatomic bonding structure and (d) Single-layer graphene scanned electron microscope image. (A higher resolution / colour version of this figure is available in the electronic copy of the article).

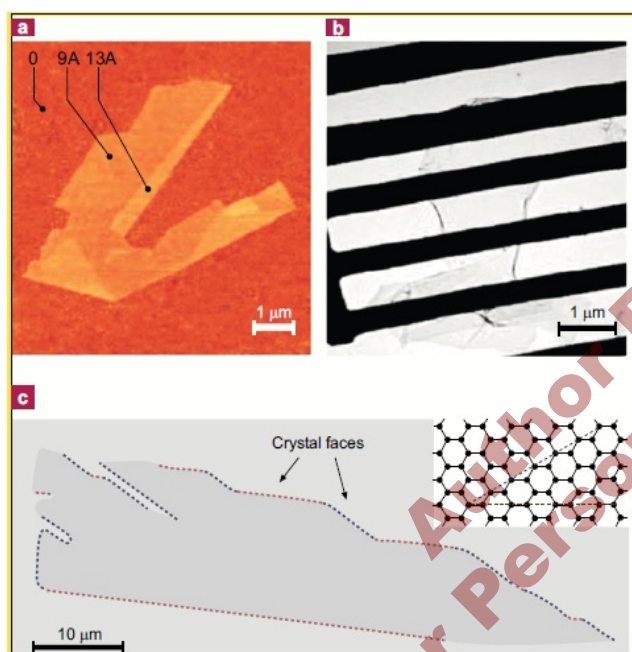


Fig. (2). (a) Atomic force microscope image of graphene, (b) A graphene sheet relies on a micrometer-size metallic scaffold. (c) Scanning electron microscope of very large graphene crystal edges. (A higher resolution / colour version of this figure is available in the electronic copy of the article).

and particularly in the case of micromechanical cleavage, it is this time-consuming implication that delays effective and full exploitation of the method [45]. A synonymous means to the micromechanical cleavage is exfoliation of graphite, which is mainly graphite oxide, that makes high production yield achievable, making the process cost-effective and scalable [46]. Exfoliation procedures have been rated high by the confirmation of its production and now industries are able to sell graphene in very large quantities [47-51].

There have been different methods for graphene synthesis since 2004 [52-54]. Chemical vapor deposition (CVD) and other surface precipitation methods have been used in recent times [55, 56]. The merit of these methods is that a

high quantity of graphene domains can be easily acquired. These methods use the ability of the transition metals to be etched by acids and the possibility of ease of transferring graphene to other substrates. However, there are still inadequate studies on the advancement of graphene in a CVD process. Various methods have been developed for the conversion of graphite into graphene. These can be classified into two main categories: (i) the top-down approach and (ii) the bottom-up approach, as can be seen in Fig. 3.

In the top-down approach, graphite exfoliating is required by overcoming van der Waals forces to expose graphene horizon layers [48, 49, 57]. It is based on disrupting graphene precursor (graphite) into atomic layers. As a result of the associated constraints of this method, surface defects and subsequent re-clustering of the separated sheets, the top-down approach yields are low, and the procedure is very tedious [58]. Meanwhile, the bottom-up approach employs carbon molecules as its building blocks, which permits the production of high-quality graphene nanoribbons and graphene nano-flakes. The reported limitation of this method is its unsuitability for the manufacturing of large surface area graphene sheets [59].

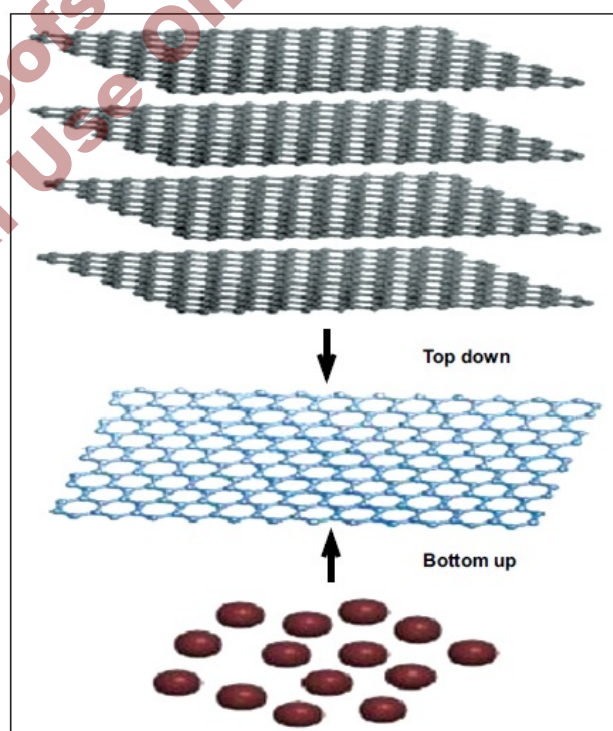


Fig. (3). Top-down and bottom-up graphene synthesis schematics. (A higher resolution / colour version of this figure is available in the electronic copy of the article).

3.1. The Top-down Approach

Graphene development has been a crux in the history of mechanical or micromechanical exfoliation methods. Studies have considered mechanical exfoliation as the main synthesis technique for the commercial production of high-quality graphene. To be precise, it delivers quality graphene films sized from about 5 to 10 μm , as given by Transmission elec-

tron microscope (TEM) and atomic force microscope (AFM) analysis (Fig. 1). Novoselov et al. [6, 48] used the same test approaches to obtain stand-alone atomic planes of mica, boron nitride, complex oxides, and dichalcogenides, but these materials in no way have attracted the attention of the research communities as graphene. The alternative method to mechanical exfoliation was proposed by Jayasena et al. [48, 60] by separating graphene from graphite source (so-called HOPG) using ultrasonic oscillation aided diamond wedge.

3.1.1. Bottom-up Approach

This is a growth from metal-carbon melts approach using graphite powder (carbon) in contact with an original metal at an elevated temperature capable of melting the metal. The temperature can decrease once the carbon is dissolved, resulting in excessive precipitation of the carbon. Consequently, various forms of carbon, such as single-layer graphene (SLG), few layers graphene (FLG), and thick graphite, would be exposed after the removal of the precipitate. Amongst proven metals suitable for this method are nickel and copper [61] and ruthenium and iridium. Nonetheless, the quality of graphene obtained from the latter is not as good as the graphene achievable by nickel and copper [41, 62]. In this process, a nickel film is heated around 900 to 1000°C in an inert chamber of argon (Fig. 4); the introduction of methane into the chamber allows carbon molecules absorption into the nickel film. Even though there are various techniques reported in the literature [48, 61], graphene synthesis on nickel films by using CVD witnessed the greatest attention.

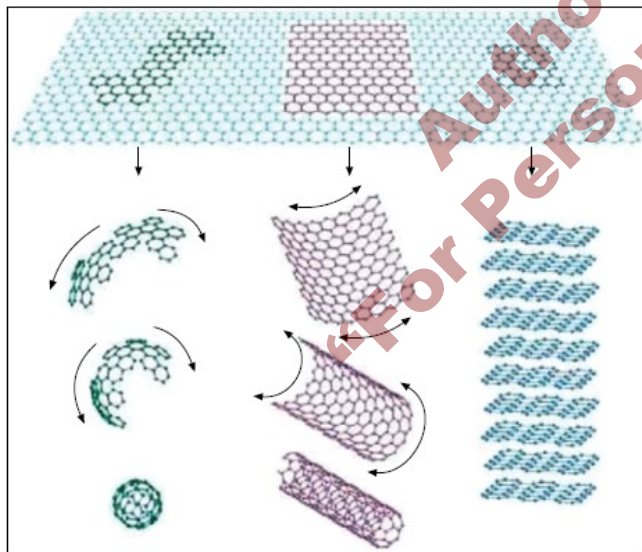


Fig. (4). Graphene (top) and related structures, fullerene (bottom left), carbon nanotubes (bottom center), and graphite (bottom right) [32]. (A higher resolution / colour version of this figure is available in the electronic copy of the article).

Graphene can serve as a building material when traced back to several forms of carbon (Geim, & Novoselov) [34, 63]. A covalent bond bonded the carbon atoms within the plane; this formed σ -bonds with three (3) bordering carbon atoms and one out-of-plane π -bond; this network of sp^2 car-

bon atoms provides a unique property to graphene. The strength of the carbon atom exceeded that of the diamond because of the presence of strong covalent in-plane bonding of the carbon atoms, whereby its high carrier mobility, room temperature ballistic conduction, and high optical transparency are characterized by its offbeat electronic structure [35]. All these promising attributes of graphene make it capable for a diversity of applications, such as devices, energy conversion and storage, field-effect transistors (FETs), tissue engineering, sensing, and membranes [64].

Graphene discovery has created an academic interest, and it has become a prospective material for today's technological needs. Its' properties have revealed some of the areas of application, for example, in graphene films, it is used as an excellent conductor, it shows good transparency in both the visible and near-infrared regions, and it has ultra-smooth surface with tunable wet ability, high chemical and thermal stabilities and flexibility for transfer between alternative substrates. Graphene can be used not only in solar cells as electrodes but also in many other optoelectronic devices [65]. Graphene film, which is prepared by a spin coating graphite oxide on quartz slice, can also be used as window electrodes for the fabrication of organic solar cells [66].

3.3. Solar Cells Using Graphene

In 2015, a hybrid of carbon nano tube and graphene (CeG-Si) was investigated by Enzheng et al. The study reported about 15.2% higher energy conversion efficiency than what is obtainable with a cell using only graphene. Fill Factor (FF) was also recommended as one of the main influential parameters of the system performance. FF has a propensity to further improve energy performance by about 25% and is highly stable in air when used as a photovoltaic cell [63]. The Chemical engineering department at Tezpur University also manufactured a highly efficient platinum-free electrode for dye-sensitized solar cells, which comprises graphene composite (polythiophene) [67]. Haoran et al. proposed a study by using multistage structure dye-sensitized solar cell (DSSC) having simple spin-coating steps, which consists of "Ag" nano-wires (AgNWs), "TiO₂" nanoparticles and graphene wrapped TiO₂ meso-porous microspheres (GTMs), as shown in Fig. 5. The graphene presence in GTMs was found to modify the bandgap of GTMs and also allows the light absorption of GTMs in the visible light region while at the same time improves the power conversion efficiency (PCE) of DSSCs. The outcome of the study revealed that a PCE of 7.42% was achieved for the DSSC co-modified by GTMs and AgNWs, which was about twice as much as that for the DSSCs only with a TiO₂ nanoparticle layer (with a PCE of 3.53%). Parameters such as V_{oc} (open circuit voltage), J_{sc} (short circuit current), FF (fill factor) and PCE (power conversion efficiency) demonstrate good long-term stability [64, 65].

3.3.2. Graphene Photoelectrodes

The photoelectrodes used in a dye-sensitized solar cell are usually obtained from TiO₂ coated transparent conductive glass or plastic substrate. Graphene has very good properties that make it unique from other nanoparticles; it has a very

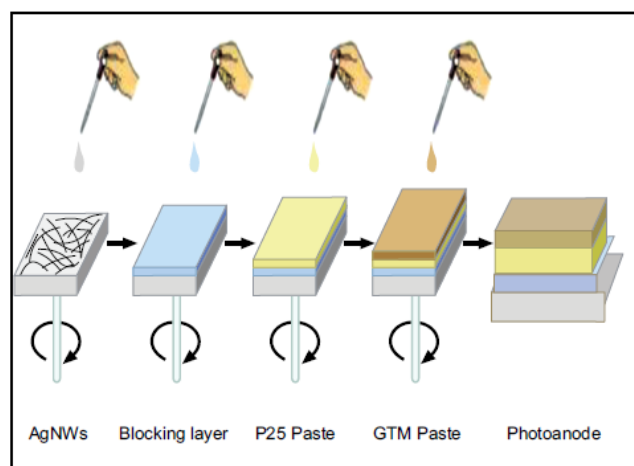


Fig. (5). Procedure for spin-coating DSSC photoanodes [68]. (A higher resolution / colour version of this figure is available in the electronic copy of the article).

good thermal stability, transparency, high electron mobility with low impedance level, which has been enticing so many researchers in smart materials design and development [40].

3.3.3. Transparent Electrode

The Indium tin oxide (ITO) nanomaterials are commonly used as transparent electrodes because of the presence of very high transmittance and conductivity properties in the visible spectrum. Despite these properties, ITO instability at high temperature and brittleness are its associated limitations. Graphene discovery may supply manufacturing industries with a better alternative to overcome the limitations of ITO. It is suitable not only because of its favorable properties but also its cost-effectiveness [69]. In 2008, Weng et al. [70] tested graphene electrodes in DSSC configuration. In Fig. 6, a solid-state dye-sensitized solar cell of spiro-OMeTAD and porous TiO is presented to illustrate the fabrication of transparent electrodes from graphene films by the exfoliation of graphite oxide for thermal management of the resultant platelets. In the study, a low work function was derived for the transparent electrode (0.26% efficiency) using graphene film of $1.8 \text{ k}\Omega/\text{sq}$ Rs and transmittance efficiency of 72% (550 nm) anode electrode. The authors claimed that the low efficiency is a result of the low quality of the graphene film utilized in the analysis [70]. Similarly, Huang et al. [71] reported the energy conversion efficiency of their system to be about 4.25%, which is just within the energy conversion range of the FTO electrode.

3.3.3.1. ZnO as Photoanode

Photoanode material plays a crucial role in sunlight harnessing (solar energy conversion) and ZnO was found to possess a similar bandgap as TiO and higher electron mobility, which makes it bolden for electrons transportation [72]. In addition to this, investigating different nanostructures and geometries (nanorods, nanosheets, nanobelt, nanotube, nanoflower, nanotetrapods and nanoparticle) contribu-

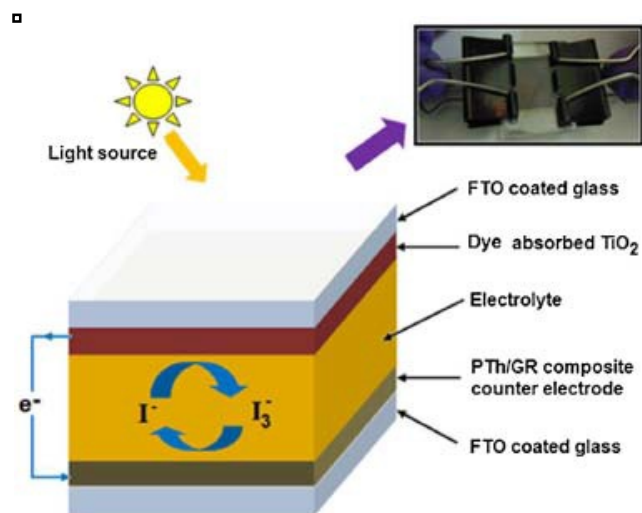


Fig. (6). PTh/GR composite DSSCs [67]. (A higher resolution / colour version of this figure is available in the electronic copy of the article).

tion to ZnO photoanode performance can enhance electro mobility optimization [73]. However, TiO₂ based solar cells can still have better efficiency than ZnO solar cells due to instability and acidity during high-charge recombination [73, 74]. When electron transfer is high, literature reported about 0.8% changeover efficiency, $3.47 \text{ mA}/\text{cm}^2$ current density (I_{sc}) and 51.7% of FF [75]. In recent years, the hydrothermal method was used to make flowered shape ZnO nano when fluorine-doped tin oxide substrate is subjected to DSSC fabrication. The result shows that ZnO of large grain size exhibits a very high open-circuit voltage (V_{OC}) and fill factor (FF) with a high recombination rate. However, the fabricated dye-sensitized solar cell has about $4.2 \text{ mA}/\text{cm}^2$ I_{sc} , 0.62 V V_{oc} , 54% of FF, and converted efficiency reaching up to 1.4% [76]. The efficiency of a fabricated dye-sensitized solar cell was also reported as $\sim 1.1\%$ coupled with $3.532 \text{ mA}/\text{cm}^2$ I_{sc} , 0.611 V , and V_{oc} , 51% [77]

Despite good optical characteristics of the low-temperature hydrothermal process of ZnO synthesis, the light-harvesting efficiency possesses a coherent absorption of a high dye by the photoanode. Kumara et al. [78, 79] proposed a spray pyrolysis method for the fabrication of dye-sensitized solar cells with dense ZnO and mesoporous layers. The result showed that, for a dense layer fabricated DSSC, an efficiency of 5.02% was obtained and 4.2% for mesoporous layer fabricated DSSC under the same condition. It implies that the surface area for the absorption is very high for DSSC with dense ZnO than that of the mesoporous layer. Other related associated parameters with dense ZnO layer are $I_{sc} = 13.68 \text{ mA}/\text{cm}^2$, 0.565 V V_{oc} and 66.3% FF, while those connected to the mesoporous layer were found to have $12.06 \text{ mA}/\text{cm}^2$ I_{sc} , 0.565 V V_{OC} , and 62.4% of FF [66].

3.4. Semiconducting Layer

Graphene may be added to a semiconductor for DSSC performance enhancement by improving charges collection. [80, 81]. Its work function of -4.4eV is between the conduction spectrum of TiO_2 and ITO [82]. Based on the theoretical studies, the irradiation of visible light can activate the valence electrons from graphene into the TiO_2 at the conductive band of graphene and TiO_2 interface [83, 84], which in turn separate electron-hole pairs. In addition, the conductive released threshold of the graphene/ TiO_2 is only at 1% volume of the graphene loading [85]. The graphene content increment in the transparent electrode is found to reduce its transmittance when it gets beyond certain thresholds. Hence, performance optimization is possible by regulating the amount of the graphene substrates [86]. The large surface area with a perfect conductivity of graphene enhances the loading and dispersion of the dye molecules. The processes of graphene have a theoretical surface area of $2630\text{ m}^2/\text{g}$; it implies that it has a very high potential of conceptual support material with an improvement in interfacial contact, even in small amounts [87]. It was reported that the graphene surface can also bind with dye molecules, such as porphyrin. Consequently, there will be a generation of photocurrent when photoirradiation experiences energy transfer [88]. Furthermore, the photoanode scattering of light can also be improved by the formation of graphene/ TiO_2 compound porous network. Then, by using graphene/ TiO_2 as the photoanode, there was an increase in efficiency by 39%, which is higher than commercial P25 TiO_2 , which is 4-7% [85]. To complete the counter-electrode and photo-anode, I- and I_3^- ion transfer electrons to the oxidized dye molecules, as shown in Fig. 7 and Fig. 8.

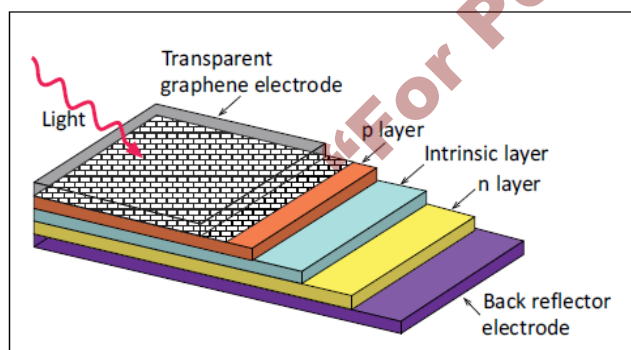


Fig. (7). Graphene-based inorganic solar cells [69]. (A higher resolution / colour version of this figure is available in the electronic copy of the article).

3.4.1. Graphene for Lithium-sulfur (Li-S) Battery

While the advent of Li-S cells in 1940 was a remarkable leap for energy-saving industries [89], there are still drawbacks associated with it. It has a short life span, high cost of production, and non-biocompatible lithium-sulphide produc-

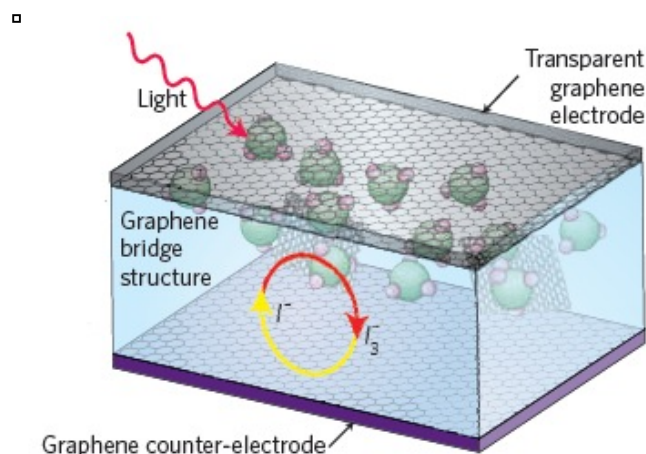


Fig. (8). Graphene dye-sensitized solar cells [69]. (A higher resolution / colour version of this figure is available in the electronic copy of the article).

tion during charge and discharge cycles [89, 90]. Graphene-enhanced electrodes in Li-S batteries provide remedies for these drawbacks [91]. As a result of the adaptability behavior, graphene is commonly used in lithium-ion batteries, Li-S batteries, supercapacitors, and other energy equipment components.

4. RECENT AND FUTURE APPLICATIONS OF GRAPHENE

The discovery and application of graphene have revolutionized smart material research premises. Yet, there are still unresolved phenomena that still need further investigations [92-95]. This section discusses the key proven areas of graphene application.

4.1. Electronic Devices

4.1.1. Transistors Designed with Flexible Graphene

The nanoscale graphene-based transistor consists of a single passage electron-interchange [96]. This type of transistor has implored extensive attention since it's incipient, and it is commercially available for various applications. The graphene-based transistor was found to utilize low voltage and be very sensitive regardless of the working temperatures [92]. These qualities position the graphene-based transistor a step ahead of the silicon-based transistor, which in turn possesses a good prospect for microchip technology. Furthermore, the intrinsic properties of graphene make it extremely flexible and foldable, among other materials. The electron mobility through graphene is substantively faster, i.e., 1000 to 10,000 times more than what is obtainable in silicon-based transistor. Although, graphene is very good in terms of electron mobility than that of silicon however, the use of pristine graphene is still limited due to electron band gap challenge.

4.1.2. Graphene Sensors

A sensor is a device that responds to some type of input signals from the physical quantities like moisture, pressure,

heat, light, motion, etc., and returns with a corresponding output, usually in the form of an electrical signal, mechanical displacement, and optical display, etc. The commonly used thermometer typifies a simple sensor for daily application. Graphene is said to be a natural sensor considering its' inherent response to optical signals and properties, having a large surface-to-volume ratio, good electrical conductivity, high carrier mobility, and high thermal conductivity [97]. Static charge phenomenon and materials strength-to-lightness ratio are basic concerns in various polymer applications in aerospace industries [98, 99]. In the very near future, graphene-enhanced materials can overcome present challenges and even provide better solar power harnessing cells for space shuttles and rovers.

4.2. Mechanism of DSSCs

Dye sensitizes solar cells belonging to the family of thin-film solar cells [101]. It relies on a semiconductor formed between a photo-sensitized and an electrolyte and photoelectrochemical system [100, 101]. The new fashion can also refer to as the Gratzel cell, which was co-invented in 1988 by Brian O'Regan and Michael Gratzel at UC Berkeley (Arora et al., 2016). DSSC possess different characteristics, that can be easily adopted using convectional roll-printing techniques, and is semi-flexible and semi-transparent, as many applications have been propounded that are not applicable to the glass-based system. Although the material used is easily affordable, a great challenge in excluding the number of expensive materials, especially platinum and ruthenium with a different kind of liquid electrolyte, contribute as a serious problem to make the cell useful for different kinds of weather conditions [102]. The mechanism of DSSC involves four major steps, absorption of light, electron injection, carrier of transportation and current collector. The steps are required for the conversion of photons into current [103]. The photon is absorbed by a photosensitizer, which allows the free movement of an electron from the ground to the excited state of the dye, whereby the absorption for most of the dye is in the range of 700 nm, which is equivalent to 1.72 eV of photon energy. The excited electron with an infinitesimal lifetime is then injected into a conduction band of nanoporous electrode beneath the excited state of the dye in order to allow the solar photon from the UV region (Kusama et al., 2009). The injected electrons are conveyed between nanoparticles and diffused along the direction of back contact (transparent conducting oxide) by the means of external circuit, to allow the electron to reach the counter electrode [104].

4.3. The Effect of Graphene on the Photoelectric Property of DSSCs

Amongst carbonaceous materials, graphene application is growing dramatically because of its exceptional thermal, mechanical, electrical, and optical properties [105]. As 2D materials (single layer materials), it has zero bandgap energy with a single molecular layered structure. In graphene, each carbon atom uses 3 of its 4 outer orbital electrons to form 3 sigma bonds. Hence, based on the distinctive properties of graphene with its interaction with TiO₂, graphene/TiO₂ composite layer, which can be applied in DSSCs, is a dynamic

way to accelerate electron transfer, impeding charge recombination and enhancing light-harvesting efficiency in the cell [106-108]. Graphene displays an impact on photoelectric properties, including a large surface area, charge carrier mobility, high conductance with a rapid transfer of an electron, which satisfy the condition for absorbing a large number of dyes in a single layer. One of the major effects of graphene of photoelectric property on DSSCs is the recombination of photo injected electrons, as well as oxidation of dyes and electrons acceptor, which reduce the efficiency of DSSCs. This problem can be solved by designing a photoanode with a remarkable impediment effect on the recombination of charge from the photo injected charge carriers to the oxidized dye and electron acceptor (Zhu et al., 2002).

4.4. Graphene Applications in Electrochemical Separations

Although there are quite a number of breakthroughs in electrochemical separations and power generations, such as fuel cells, electro dialysis, bio-chemical extraction and separation [109], yet unresolved limitations in this area of research (over limiting currents, electro-osmosis, cell materials having low conductivities specifically for membranes and electrodes) may be addressed via explorative investigation of graphene promising properties [110-113]. Solar power utilization for electrochemical cells has also been recommended in the literature. Therefore, incorporating graphene into the electrochemical cell will invariably ameliorate solar and electrolytic cells' performance optimization. Oil recovery is another attractive area of interest for researchers and graphene has been reported to be a potential material for electromagnetic field-assisted oil recovery technique, Enhanced Oil Recovery (EOR) applications [114-117].

CONCLUSION

In this review, graphene synthesis, drawbacks, and potential directions in promoting graphene practical configuration are succinctly discussed. The following conclusions are derived:

(1) Mechanical exfoliation synthesis technique reported delivering quality graphene films sized from about 5 to 10 μm ; graphene-TiO₂ hybridization was found to possess efficiency acclivity as high as 39%.

(2) Graphene layers number, defects, and bandgap structure are the fundamental performance influential parameters within the graphene inter-lattice structure. This is due to graphene surface area, which can reach up to about 2630-900 m²/g, while carbon-black and carbon-nano-tube surface area capability is around 1000-100 m²/g. Also, the Fill Factor (FF) is recommended as one of the main influential parameters of the system performance.

(3) Reported techniques of synthesizing ZnO₂ transparent electrodes are found to have changed over the efficiency of about 0.8, 1.1, and about 4.2-5.2% for CBC, DSSC, and mesoporous layer DSSC, respectively.

Finally, graphene's relevance to the ongoing industrial revolutions can never be overlooked, and the authors of this work want to believe that in not too distant future, graphene

materials' understanding would further enhance their real-time application to meet a broad industrial range of needs.

CONSENT FOR PUBLICATION

Not applicable.

FUNDING

None.

CONFLICT OF INTEREST

The authors declare no conflict of interest, financial or otherwise.

ACKNOWLEDGEMENTS

Declared none.

REFERENCES

- [1] Hasin, P.; Alpuche-Aviles, M.A.; Wu, Y. Electrocatalytic activity of graphene multilayers toward I⁻/I₃⁻: Effect of preparation conditions and polyelectrolyte modification. *J. Phys. Chem. C*, **2010**, *114*, 15857-15861. <http://dx.doi.org/10.1021/jp106130v>
- [2] Olalekan, S.; Abdullahi, M.; Olabisi, A. Modeling of solar radiation using artificial neural network for renewable energy application. *J. Appl. Phys.*, **2018**, *10*, 6-12.
- [3] Yang, G.; Li, L.; Lee, W.B.; Ng, M.C. Structure of graphene and its disorders: A review. *Sci. Technol. Adv. Mater.*, **2018**, *19*(1), 613-648. <http://dx.doi.org/10.1080/14686996.2018.1494493> PMID: 30181789
- [4] Morozov, S.V.; Novoselov, K.S.; Katsnelson, M.I.; Schedin, F.; Elias, D.C.; Jaszczak, J.A.; Geim, A.K. Giant intrinsic carrier mobilities in graphene and its bilayer. *Phys. Rev. Lett.*, **2008**, *100*(1), 016602. <http://dx.doi.org/10.1103/PhysRevLett.100.016602> PMID: 18232798
- [5] Vellei, M.; Herrera, M.; Fosas, D.; Natarajan, S. The influence of relative humidity on adaptive thermal comfort. *Build. Environ.*, **2017**, *124*, 171-185. <http://dx.doi.org/10.1016/j.buildenv.2017.08.005>
- [6] Vellei, M.; Herrera, M.; Fosas, D.; Natarajan, S.V. 2017 #836], "The influence of relative humidity on adaptive thermal comfort. *Build. Environ.*, **2017**, *124*, 171-185. <http://dx.doi.org/10.1016/j.buildenv.2017.08.005>
- [7] Surajudeen, S.; Yahya, N.; Soleimani, H.; Musa, A.A.; Afeez, Y.; Rostami, A. Effect of adsorption on saturated sandstone within electric double layer on solid/liquid inter-phase. *Petroleum & Coal*, **2019**, *61*, .
- [8] Aliu, T.; Sakidin, H.; Yahya, N.; Sikiru, S.; Ali, A. M. Dynamics of nanoparticles propagation in porous media. **2019**.
- [9] Afeez, Y.; Yahya, N.; Nyuk, C. M.; Al-qaseem, B.; Qureshi, S.; Sikiru, Investigation on nanoparticles effect on interfacial forces for enhanced oil recovery. **2019**.
- [10] Roy-Mayhew, J.D.; Bozym, D.J.; Punckt, C.; Aksay, I.A. Functionalized graphene as a catalytic counter electrode in dye-sensitized solar cells. *ACS Nano*, **2010**, *4*(10), 6203-6211. <http://dx.doi.org/10.1021/nn1016428> PMID: 20939517
- [11] Kavan, L.; Yum, J.H.; Grätzel, M. Optically transparent cathode for dye-sensitized solar cells based on graphene nanoplatelets. *ACS Nano*, **2011**, *5*(1), 165-172. <http://dx.doi.org/10.1021/nn102353h> PMID: 21126092
- [12] Yusuff, A.O.; Yahya, N.; Zakariya, M.A.; Sikiru, S. Investigations of graphene impact on oil mobility and physicochemical interaction with sandstone surface. *J. Petrol. Sci. Eng.*, **2020**, 108250.
- [13] Yusuf, J.Y.; Soleimani, H.; Sanusi, Y.K.; Adebayo, L.L.; Sikiru, S.; Wahaab, F.A. Recent advances and prospect of cobalt based microwave absorbing materials. *Ceram. Int.*, **2020**. <http://dx.doi.org/10.1016/j.ceramint.2020.07.244>
- [14] Gao, X.; Jang, J.; Nagase, S. Hydrazine and thermal reduction of graphene oxide: Reaction mechanisms, product structures, and reaction design. *J. Phys. Chem. C*, **2010**, *114*, 832-842. <http://dx.doi.org/10.1021/jp909284g>
- [15] Mattevi, C.; Eda, G.; Agnoli, S.; Miller, S. KAM khoyan, O. Celik, D. Mastrogiovanni, G. Granozzi, E. Garfunkel, and M. Chhowalla. *Adv. Funct. Mater.*, **2009**, *9*, 2577. <http://dx.doi.org/10.1002/adfm.200900166>
- [16] Bolotin, K.I.; Sikes, K.J.; Jiang, Z.; Klima, M.; Fudenberg, G.; Hone, J. Ultrahigh electron mobility in suspended graphene. *Solid State Commun.*, **2008**, *146*, 351-355. <http://dx.doi.org/10.1016/j.ssc.2008.02.024>
- [17] Sanusi, Y.; Fajinmi, G.; Babatunde, E. Effects of ambient temperature on the performance of a photovoltaic solar system in a tropical area. *Pac. J. Sci. Technol.*, **2011**, *12*, 176-180.
- [18] Sanusi, Y.K.; Abisoye, S.G. Estimation of solar radiation at Ibadan, Nigeria. *Journal of Emerging Trends in Engineering and Applied Sciences*, **2011**, *2*, 701-705.
- [19] Sanusi, Y. The performance of amorphous silicon PV system under Harmattan dust conditions in a tropical area. *Pac. J. Sci. Technol.*, **2012**, *13*, 168-175.
- [20] Sanusi, Y.; Abisoye, S. Estimation of wind energy potential in Southwestern Nigeria. *Pac. J. Sci. Technol.*, **2011**, *12*, 160-166.
- [21] Sanusi, Y.; Abisoye, S.; Awodugba, A. Application of neural networks for predicting the optimal sizing parameters of stand-alone photovoltaic systems. *SOP Trans Appl Phys.*, **2014**, *1*, 1-5.
- [22] Awodugba, A.; Sanusi, Y.; Ajayi, J. Photovoltaic solar cell simulation of shokley diode parameters in matlab. *Int. J. Phys. Sci.*, **2013**, *8*, 1193-1200.
- [23] Zhang, H.; Wang, W.; Liu, H.; Wang, R.; Chen, Y.; Wang, Z. Effects of TiO₂ film thickness on photovoltaic properties of dye-sensitized solar cell and its enhanced performance by graphene combination. *Mater. Res. Bull.*, **2014**, *49*, 126-131. <http://dx.doi.org/10.1016/j.materresbull.2013.08.058>
- [24] Saadi, S.; Nazari, B. Recent developments and applications of nanocomposites in solar cells: A review. *Journal of Composites and Compounds*, **2019**, *1*, 41-50. <http://dx.doi.org/10.29252/jcc.1.1.7>
- [25] Wang, X.; Li, Y.; Song, P.; Ma, F.; Yang, Y. Effect of graphene between photoanode and sensitizer on the intramolecular and intermolecular electron transfer process. *Phys. Chem. Chem. Phys.*, **2020**, *22*(11), 6391-6400. <http://dx.doi.org/10.1039/C9CP06543A> PMID: 32142089
- [26] Sen, T.; Shimpi, N.G.; Mishra, S.; Sharma, R. Polyaniline/ γ -Fe₂O₃ nanocomposite for room temperature LPG sensing. *Sens. Actuators B Chem.*, **2014**, *190*, 120-126. <http://dx.doi.org/10.1016/j.snb.2013.07.091>
- [27] Sanusi, Y.; Asafa, T.; Kazeem, A. Optimization of TiO₂ based henna dye sensitized solar cell using Grey-Taguchi technique. *International Journal Of Renewable Energy Research*, **2016**, *6*, 1119-1128.
- [28] Leong, W.S.; Nai, C.T.; Thong, J.T. What does annealing do to metal-graphene contacts? *Nano Lett.*, **2014**, *14*(7), 3840-3847. <http://dx.doi.org/10.1021/nl500999f> PMID: 24912079
- [29] Xu, Y.; Bai, H.; Lu, G.; Li, C.; Shi, G. Flexible graphene films via the filtration of water-soluble noncovalent functionalized graphene sheets. *J. Am. Chem. Soc.*, **2008**, *130*(18), 5856-5857. <http://dx.doi.org/10.1021/ja800745y> PMID: 18399634
- [30] Tung, V.C.; Chen, L.-M.; Allen, M.J.; Wassei, J.K.; Nelson, K.; Kaner, R.B.; Yang, Y. Low-temperature solution processing of graphene-carbon nanotube hybrid materials for high-performance transparent conductors. *Nano Lett.*, **2009**, *9*(5), 1949-1955. <http://dx.doi.org/10.1021/nl9001525> PMID: 19361207
- [31] Zhang, Y.; Small, J.P.; Pontius, W.V.; Kim, P. Fabrication and electric-field-dependent transport measurements of mesoscopic graphite devices. *Appl. Phys. Lett.*, **2005**, *86*, 073104. <http://dx.doi.org/10.1063/1.1862334>
- [32] Chen, J.-H.; Jang, C.; Xiao, S.; Ishigami, M.; Fuhrer, M.S. Intrinsic and extrinsic performance limits of graphene devices on SiO₂. *Nat. Nanotechnol.*, **2008**, *3*(4), 206-209. <http://dx.doi.org/10.1038/nnano.2008.58> PMID: 18654504

- [33] Geim, A.K.; Novoselov, K.S. The rise of graphene. *Nanoscience and technology: A collection of reviews from nature journals*; World Scientific, **2010**, pp. 11-19.
- [34] Weatherup, R.S.; Bayer, B.C.; Blume, R.; Ducati, C.; Baetz, C.; Schlögl, R.; Hofmann, S. *In situ* characterization of alloy catalysts for low-temperature graphene growth. *Nano Lett.*, **2011**, *11*(10), 4154-4160.
<http://dx.doi.org/10.1021/nl202036y> PMID: 21905732
- [35] Novoselov, K.S.; Geim, A.K.; Morozov, S.V.; Jiang, D.; Zhang, Y.; Dubonos, S.V. Electric field effect in atomically thin carbon films. *science*, **2004**, *306*, 666-669.
<http://dx.doi.org/10.1126/science.1102896>
- [36] Novoselov, K.S.; Geim, A.K.; Morozov, S.V.; Jiang, D.; Katsnelson, M.I.; Grigorieva, I. Two-dimensional gas of massless Dirac fermions in graphene. *nature*, **2005**, *438*, 197-200.
<http://dx.doi.org/10.1038/nature04233>
- [37] Wu, J.; Becerril, H.A.; Bao, Z.; Liu, Z.; Chen, Y.; Peumans, P. Organic solar cells with solution-processed graphene transparent electrodes. *Appl. Phys. Lett.*, **2008**, *92*, 237.
<http://dx.doi.org/10.1063/1.2924771>
- [38] Vollmer, A.; Feng, X.; Wang, X.; Zhi, L.; Müllen, K.; Koch, N. Electronic and structural properties of graphene-based transparent and conductive thin film electrodes. *Appl. Phys., A Mater. Sci. Process.*, **2009**, *94*, 1-4.
<http://dx.doi.org/10.1007/s00339-008-4931-2>
- [39] Coraux, J.; N'Diaye, A.T.; Busse, C.; Michely, T. Structural coherence of graphene on Ir(111). *Nano Lett.*, **2008**, *8*(2), 565-570.
<http://dx.doi.org/10.1021/nl0728874> PMID: 18189442
- [40] Cao, X.; Yin, Z.; Zhang, H. Three-dimensional graphene materials: Preparation, structures and application in supercapacitors. *Energy Environ. Sci.*, **2014**, *7*, 1850-1865.
<http://dx.doi.org/10.1039/C4EE00050A>
- [41] Sutter, P.W.; Flege, J.-I.; Sutter, E.A. Epitaxial graphene on ruthenium. *Nat. Mater.*, **2008**, *7*(5), 406-411.
<http://dx.doi.org/10.1038/nmat2166> PMID: 18391956
- [42] Becerril, H.A.; Mao, J.; Liu, Z.; Stoltenberg, R.M.; Bao, Z.; Chen, Y. Evaluation of solution-processed reduced graphene oxide films as transparent conductors. *ACS Nano*, **2008**, *2*(3), 463-470.
<http://dx.doi.org/10.1021/nm700375n> PMID: 19206571
- [43] Dato, A.; Radmilovic, V.; Lee, Z.; Phillips, J.; Frenklach, M. Substrate-free gas-phase synthesis of graphene sheets. *Nano Lett.*, **2008**, *8*(7), 2012-2016.
<http://dx.doi.org/10.1021/nl8011566> PMID: 18529034
- [44] Reina, A.; Jia, X.; Ho, J.; Nezich, D.; Son, H.; Bulovic, V.; Dresselhaus, M.S.; Kong, J. Large area, few-layer graphene films on arbitrary substrates by chemical vapor deposition. *Nano Lett.*, **2009**, *9*(1), 30-35.
<http://dx.doi.org/10.1021/nl801827v> PMID: 19046078
- [45] Verdejo, R.; Bernal, M.M.; Romasanta, L.J.; Lopez-Manchado, M.A. Graphene filled polymer nanocomposites. *J. Mater. Chem.*, **2011**, *21*, 3301-3310.
<http://dx.doi.org/10.1039/C0JM02708A>
- [46] Park, S.; Ruoff, R. *Nat Nanotechnol* **4**, **2009**, 217e24.
- [47] Segal, M. Selling graphene by the ton. *Nat. Nanotechnol.*, **2009**, *4*(10), 612-614.
<http://dx.doi.org/10.1038/nnano.2009.279> PMID: 19809441
- [48] Surajudeen, S.; Rostami, A.; Soleimani, H.; Yahya, N.; Afeez, Y.; Oluwaseyi, A. Graphene: Outlook in the enhance oil recovery (EOR). *J. Mol. Liq.*, **2020**, 114519.
- [49] Yahya, N.; Sikiru, S.; Rostami, A.; Soleimani, H.; Alqasem, B.; Qureishi, S. Percolation threshold of multiwall carbon nanotube-PVDF composite for electromagnetic wave propagation. *Nano Express*, **2020**, *1*, 010060.
<http://dx.doi.org/10.1088/2632-959X/ab9d69>
- [50] Alqasem, B.; Sikiru, S.; Ali, E. M.; Rostami, A.; Ganeson, M.; Nyuk, C. M. Effect of electromagnetic energy on net spin orientation of nanocatalyst for enhanced green urea synthesis. *Journal of materials research and technology*, **2020**.
- [51] Jiang, M.; Ren, Z.; Lu, B.; Guo, T.; Wan, L.; Zhang, Y. Low-repetition-rate high-energy passively Q-switched Nd: YAG solid laser based on graphene saturable absorber operating at 1064nm. *Curr. Nanosci.*, **2012**, *8*, 60-63.
<http://dx.doi.org/10.2174/1573413711208010060>
- [52] Marchini, S.; Günther, S.; Witterlin, J. Scanning tunneling microscopy of graphene on Ru (0001). *Phys. Rev. B*, **2007**, *76*, 075429.
<http://dx.doi.org/10.1103/PhysRevB.76.075429>
- [53] Esfe, M.H.; Wongwises, S.; Esfandeh, S.; Alirezaie, A. Development of a new correlation and post processing of heat transfer coefficient and pressure drop of functionalized COOH MWCNT nanofluid by artificial neural network. *Curr. Nanosci.*, **2018**, *14*, 104-112.
<http://dx.doi.org/10.2174/1573413713666170913122649>
- [54] Durán, N.; Seabra, A. Biogenic synthesized Ag/Au nanoparticles: Production, characterization, and applications. *Curr Nanosci.*, **2018**, *14*, pp. 82-94.
- [55] Vázquez de Parga, A.L.; Calleja, F.; Borca, B.; Passeggi, M.C., Jr; Hinarejos, J.J.; Guinea, F.; Miranda, R. Periodically rippled graphene: Growth and spatially resolved electronic structure. *Phys. Rev. Lett.*, **2008**, *100*(5), 056807.
<http://dx.doi.org/10.1103/PhysRevLett.100.056807> PMID: 18352412
- [56] Edwards, R.S.; Coleman, K.S. Graphene synthesis: Relationship to applications. *Nanoscale*, **2013**, *5*(1), 38-51.
<http://dx.doi.org/10.1039/C2NR32629A> PMID: 23160190
- [57] Na, M.Y.; Lee, S.-M.; Kim, D.H.; Chang, H.J. Dark-field transmission electron microscopy imaging technique to visualize the local structure of two-dimensional material; graphene. *Applied Microscopy*, **2015**, *45*, 23-31.
<http://dx.doi.org/10.9729/AM.2015.45.1.23>
- [58] MacKenzie, K.J.; Dumens, O.M.; See, C.H.; Harris, A.T. Large-scale carbon nanotube synthesis. *Recent Pat. Nanotechnol.*, **2008**, *2*(1), 25-40.
<http://dx.doi.org/10.2174/187221008783478617> PMID: 19076041
- [59] Randviir, E.P.; Brownson, D.A.; Banks, C.E. A decade of graphene research: Production, applications and outlook. *Mater. Today*, **2014**, *17*, 426-432.
<http://dx.doi.org/10.1016/j.mattod.2014.06.001>
- [60] Jayasena, B.; Subbiah, S. A novel mechanical cleavage method for synthesizing few-layer graphenes. *Nanoscale Res. Lett.*, **2011**, *6*(1), 95.
<http://dx.doi.org/10.1186/1556-276X-6-95> PMID: 21711598
- [61] Amini, S.; Garay, J.; Liu, G.; Balandin, A.A.; Abbaschian, R. Growth of large-area graphene films from metal-carbon melts. *J. Appl. Phys.*, **2010**, *108*, 094321.
<http://dx.doi.org/10.1063/1.3498815>
- [62] Pletkosić, I.; Kralj, M.; Pervan, P.; Brako, R.; Coraux, J.; N'diaye, A.T.; Busse, C.; Michely, T. Dirac cones and minigaps for graphene on Ir(111). *Phys. Rev. Lett.*, **2009**, *102*(5), 056808.
<http://dx.doi.org/10.1103/PhysRevLett.102.056808> PMID: 19257540
- [63] Bunch, J.S.; Verbridge, S.S.; Alden, J.S.; van der Zande, A.M.; Parpia, J.M.; Craighead, H.G.; McEuen, P.L. Impermeable atomic membranes from graphene sheets. *Nano Lett.*, **2008**, *8*(8), 2458-2462.
<http://dx.doi.org/10.1021/nl801457b> PMID: 18630972
- [64] Yang, Y.; Liu, R.; Wu, J.; Jiang, X.; Cao, P.; Hu, X.; Pan, T.; Qiu, C.; Yang, J.; Song, Y.; Wu, D.; Su, Y. Bottom-up fabrication of graphene on silicon/silica substrate via a facile soft-hard template approach. *Sci. Rep.*, **2015**, *5*, 13480.
<http://dx.doi.org/10.1038/srep13480> PMID: 26311022
- [65] Tiwari, S.K.; Mishra, R.K.; Ha, S.K.; Huczko, A. Evolution of graphene oxide and graphene: From imagination to industrialization. *ChemNanoMat*, **2018**, *4*, 598-620.
<http://dx.doi.org/10.1002/cnma.201800089>
- [66] Chen, T.; Hu, W.; Song, J.; Guai, G.H.; Li, C.M. Interface functionalization of photoelectrodes with graphene for high performance dye-sensitized solar cells. *Adv. Funct. Mater.*, **2012**, *22*, 5245-5250.
<http://dx.doi.org/10.1002/adfm.201201126>
- [67] Yan, H.; Wang, J.; Feng, B.; Duan, K.; Weng, J. Graphene and Ag nanowires co-modified photoanodes for high-efficiency dye-sensitized solar cells. *Sol. Energy*, **2015**, *122*, 966-975.
<http://dx.doi.org/10.1016/j.solener.2015.10.026>
- [68] Zhang, Y.; Zhang, L.; Zhou, C. Review of chemical vapor deposition of graphene and related applications. *Acc. Chem. Res.*, **2013**, *46*(10), 2329-2339.
<http://dx.doi.org/10.1021/ar300203n> PMID: 23480816

- [69] Bonaccorso, F.; Sun, Z.; Hasan, T.; Ferrari, A. Graphene photonics and optoelectronics. *Nat. Photonics*, **2010**, *4*, 611. <http://dx.doi.org/10.1038/nphoton.2010.186>
- [70] Wang, X.; Zhi, L.; Müllen, K. Transparent, conductive graphene electrodes for dye-sensitized solar cells. *Nano Lett.*, **2008**, *8*(1), 323-327. <http://dx.doi.org/10.1021/nl072838r> PMID: 18069877
- [71] Bi, H.; Sun, S.; Huang, F.; Xie, X.; Jiang, M. Direct growth of few-layer graphene films on SiO₂ substrates and their photovoltaic applications. *J. Mater. Chem.*, **2012**, *22*, 411-416. <http://dx.doi.org/10.1039/C1JM14778A>
- [72] Sharifi, N.; Tajabadi, F.; Taghavinia, N. Recent developments in dye-sensitized solar cells. *ChemPhysChem*, **2014**, *15*(18), 3902-3927. <http://dx.doi.org/10.1002/cphc.201402299> PMID: 25277957
- [73] Zhang, Q.; Dandeneau, C.S.; Zhou, X.; Cao, G. ZnO nanostructures for dye-sensitized solar cells. *Adv. Mater.*, **2009**, *21*, 4087-4108. <http://dx.doi.org/10.1002/adma.200803827>
- [74] Raj, C.C.; Prasanth, R. A critical review of recent developments in nanomaterials for photoelectrodes in dye sensitized solar cells. *J. Power Sources*, **2016**, *317*, 120-132. <http://dx.doi.org/10.1016/j.jpowsour.2016.03.016>
- [75] Boda, M.A.; Çırak, B.B.; Demir, Z.; Çırak, Ç. Facile synthesis of hybrid ZnO nanostructures by combined electrodeposition and chemical bath deposition for improved performance of dye-sensitized solar cell. *Mater. Lett.*, **2019**, *248*, 143-145. <http://dx.doi.org/10.1016/j.matlet.2019.04.023>
- [76] Shittu, H.; Bello, I.; Kareem, M.; Awodele, M.; Sanusi, Y.; Adedokun, O. Recent developments on the photoanodes employed in dye-sensitized solar cell. *IOP conference series: Materials science and engineering*, **2020**, p. 012019.
- [77] Umar, A.; Ibrahim, A.A. Fabrication and characterization of dye-sensitized solar cells based on flower shaped ZnO nanostructures. *J. Nanosci. Nanotechnol.*, **2018**, *18*(5), 3697-3701. <http://dx.doi.org/10.1166/jnn.2018.14657> PMID: 29442886
- [78] Zhang, L.; Konno, A. Development of flexible dye-sensitized solar cell based on predeyed zinc oxide nanoparticle. *Int. J. Electrochem. Sci.*, **2018**, *13*, 344-352. <http://dx.doi.org/10.20964/2018.01.07>
- [79] Kumara, G.; Deshapriya, U.; Ranasinghe, C.; Jayaweera, E.; Rajapakse, R. Efficient dye-sensitized solar cells from mesoporous zinc oxide nanostructures sensitized by N719 dye. *J. Semicond.*, **2018**, *39*, 033005. <http://dx.doi.org/10.1088/1674-4926/39/3/033005>
- [80] Ramanathan, T.; Abdala, A.A.; Stankovich, S.; Dikin, D.A.; Herrera-Alonso, M.; Piner, R.D.; Adamson, D.H.; Schniepp, H.C.; Chen, X.; Ruoff, R.S.; Nguyen, S.T.; Aksay, I.A.; Prud'Homme, R.K.; Brinson, L.C. Functionalized graphene sheets for polymer nanocomposites. *Nat. Nanotechnol.*, **2008**, *3*(6), 327-331. <http://dx.doi.org/10.1038/nnano.2008.96> PMID: 18654541
- [81] Wang, H.; Leonard, S.L.; Hu, Y.H. Promoting effect of graphene on dye-sensitized solar cells. *Ind. Eng. Chem. Res.*, **2012**, *51*, 10613-10620. <http://dx.doi.org/10.1021/ie300563h>
- [82] Tang, Y.-B.; Lee, C.-S.; Xu, J.; Liu, Z.-T.; Chen, Z.-H.; He, Z.; Cao, Y.L.; Yuan, G.; Song, H.; Chen, L.; Luo, L.; Cheng, H.M.; Zhang, W.J.; Bello, I.; Lee, S.T. Incorporation of graphenes in nanostructured TiO₂ films via molecular grafting for dye-sensitized solar cell application. *ACS Nano*, **2010**, *4*(6), 3482-3488. <http://dx.doi.org/10.1021/nn100449w> PMID: 20455548
- [83] Du, A.; Ng, Y.H.; Bell, N.J.; Zhu, Z.; Amal, R.; Smith, S.C. Hybrid graphene/titania nanocomposite: Interface charge transfer, hole doping, and sensitization for visible light response. *J. Phys. Chem. Lett.*, **2011**, *2*(8), 894-899. <http://dx.doi.org/10.1021/jz2002698> PMID: 26295625
- [84] Ajadi, D.; Sanusi, Y. Effect of relative humidity on oven temperature of locally design solar carbinet dryer. *Global journal of science frontier research physics and space science*, **2013**, *13*
- [85] Liang, J.; Zhang, G.; Yang, J.; Sun, W.; Shi, M. TiO₂ hierarchical nanostructures: Hydrothermal fabrication and application in dye-sensitized solar cells. *AIP Adv.*, **2015**, *5*, 017141. <http://dx.doi.org/10.1063/1.4906988>
- [86] Yang, N.; Zhai, J.; Wang, D.; Chen, Y.; Jiang, L. Two-dimensional graphene bridges enhanced photoinduced charge transport in dye-sensitized solar cells. *ACS Nano*, **2010**, *4*(2), 887-894. <http://dx.doi.org/10.1021/nn901660v> PMID: 20088539
- [87] Peigney, A.; Laurent, C.; Flahaut, E.; Bacsca, R.; Rousset, A. Specific surface area of carbon nanotubes and bundles of carbon nanotubes. *Carbon*, **2001**, *39*, 507-514. [http://dx.doi.org/10.1016/S0008-6223\(00\)00155-X](http://dx.doi.org/10.1016/S0008-6223(00)00155-X)
- [88] Wojcik, A.; Kamat, P.V. Reduced graphene oxide and porphyrin. An interactive affair in 2-D. *ACS Nano*, **2010**, *4*(11), 6697-6706. <http://dx.doi.org/10.1021/nn102185q> PMID: 21028793
- [89] Bogue, R. Graphene sensors: A review of recent developments. *Sens. Rev.*, **2014**. <http://dx.doi.org/10.1108/SR-03-2014-631>
- [90] Song, J.; Yu, Z.; Gordin, M.L.; Wang, D. Advanced sulfur cathode enabled by highly crumpled nitrogen-doped graphene sheets for high-energy-density lithium-sulfur batteries. *Nano Lett.*, **2016**, *16*(2), 864-870. <http://dx.doi.org/10.1021/acs.nanolett.5b03217> PMID: 26709841
- [91] Hong, J.Y.; Jung, Y.; Park, D.-W.; Chung, S.; Kim, S. Synthesis and electrochemical analysis of electrode prepared from zeolitic imidazolate framework (ZIF)-67/graphene composite for lithium sulfur cells. *Electrochim. Acta*, **2018**, *259*, 1021-1029. <http://dx.doi.org/10.1016/j.electacta.2017.11.016>
- [92] He, S.; Qian, Y.; Liu, K.; Macosko, C.W.; Stein, A. Modified-graphene-oxide-containing styrene masterbatches for thermosets. *Ind. Eng. Chem. Res.*, **2017**, *56*, 11443-11450. <http://dx.doi.org/10.1021/acs.iecr.7b02583>
- [93] Neto, A.C.; Guinea, F.; Peres, N.M.; Novoselov, K.S.; Geim, A.K. The electronic properties of graphene. *Rev. Mod. Phys.*, **2009**, *81*, 109. <http://dx.doi.org/10.1103/RevModPhys.81.109>
- [94] Amiri, A.; Sadri, R.; Shanbedi, M.; Ahmadi, G.; Chew, B.; Kazi, S.N. Performance dependence of thermosyphon on the functionalization approaches: An experimental study on thermo-physical properties of graphene nanoplatelet-based water nanofluids. *Energy Convers. Manage.*, **2015**, *92*, 322-330. <http://dx.doi.org/10.1016/j.enconman.2014.12.051>
- [95] Blaschke, B. M.; Lottner, M.; Drieschner, S.; Calia, A. B.; Stoiber, K.; Rousseau, L. Flexible graphene transistors for recording cell action potentials. *2D Materials*, **2016**, *3*, 025007. <http://dx.doi.org/10.1088/2053-1583/3/2/025007>
- [96] Xu, J.; Gu, Z.; Yang, W.; Wang, Q.; Zhang, X. Graphene-based nanoscale vacuum channel transistor. *Nanoscale Res. Lett.*, **2018**, *13*(1), 311. <http://dx.doi.org/10.1186/s11671-018-2736-6> PMID: 30288627
- [97] Zhao, Y.; Li, X.-g.; Zhou, X.; Zhang, Y.-n. Review on the graphene based optical fiber chemical and biological sensors. *Sens. Actuators B Chem.*, **2016**, *231*, 324-340. <http://dx.doi.org/10.1016/j.snb.2016.03.026>
- [98] Yadav, R.; Tirumali, M.; Wang, X.; Naebe, M.; Kandasubramanian, B. Polymer composite for antistatic application in aerospace. *Defence Technology*, **2020**, *16*, 107-118. <http://dx.doi.org/10.1016/j.dt.2019.04.008>
- [99] Moupfouma, F. Electrostatic discharge phenomenon: A potential threat to aircraft safety. *SAE technical paper*, **2007**, 0148-7191. <http://dx.doi.org/10.4271/2007-01-3833>
- [100] Liu, X.; Chen, T.; Chu, H.; Niu, L.; Sun, Z.; Pan, L. Fe₂O₃-reduced graphene oxide composites synthesized via microwave-assisted method for sodium ion batteries. *Electrochim. Acta*, **2015**, *166*, 12-16. <http://dx.doi.org/10.1016/j.electacta.2015.03.081>
- [101] Fitra, M.; Daut, I.; Irwanto, M.; Gomes, N.; Irwan, Y. Effect of TiO₂ thickness dye solar cell on charge generation. *Energy Procedia*, **2013**, *36*, 278-286. <http://dx.doi.org/10.1016/j.egypro.2013.07.032>
- [102] Tributsch, H. Dye sensitization solar cells: A critical assessment of the learning curve. *Coord. Chem. Rev.*, **2004**, *248*, 1511-1530. <http://dx.doi.org/10.1016/j.ccr.2004.05.030>
- [103] Zhuge, Z.; Liu, X.; Chen, T.; Gong, Y.; Li, C.; Niu, L. Highly efficient photocatalytic degradation of different hazardous contaminants by CaIn₂S₄-Ti₃C₂Tx Schottky heterojunction: An experimental and mechanism study. *Chem. Eng. J.*, **2020**, 127838. <http://dx.doi.org/10.1016/j.cej.2020.127838>

- [104] Ren, Z.; Liu, X.; Zhuge, Z.; Gong, Y.; Sun, C.Q. MoSe₂/ZnO/ZnSe hybrids for efficient Cr (VI) reduction under visible light irradiation. *Chin. J. Catal.*, **2020**, *41*, 180-187.
[http://dx.doi.org/10.1016/S1872-2067\(19\)63484-4](http://dx.doi.org/10.1016/S1872-2067(19)63484-4)
- [105] Wei, L.; Chen, S.; Yang, Y.; Dong, Y.; Song, W.; Fan, R. Effect of graphene/TiO₂ composite layer on the performance of dye-sensitized solar cells. *J. Nanosci. Nanotechnol.*, **2018**, *18*(2), 976-983.
<http://dx.doi.org/10.1166/jnn.2018.14186> PMID: 29448522
- [106] Nair, R.R.; Blake, P.; Grigorenko, A.N.; Novoselov, K.S.; Booth, T.J.; Stauber, T.; Peres, N.M.; Geim, A.K. Fine structure constant defines visual transparency of graphene. *Science*, **2008**, *320*(5881), 1308-1308.
<http://dx.doi.org/10.1126/science.1156965> PMID: 18388259
- [107] Stankovich, S.; Dikin, D.; Dommett, G.; Kohlhaas, K.; Zimney, E.; Stach, E. ST 22 Nguyen. *RS Ruoff, graphene-based composite materials, nature*, **2006**, *442*, 7100.
- [108] Li, D.; Kaner, R.B. Materials science. Graphene-based materials. *Science*, **2008**, *320*(5880), 1170-1171.
<http://dx.doi.org/10.1126/science.1158180> PMID: 18511678
- [109] Alzate, M.; Muñoz, R.; Rogalla, F.; Fdz-Polanco, F.; Pérez-Elvira, S. Biochemical methane potential of microalgae biomass after lipid extraction. *Chem. Eng. J.*, **2014**, *243*, 405-410.
<http://dx.doi.org/10.1016/j.cej.2013.07.076>
- [110] Anjum, U.; Khan, T.S.; Agarwal, M.; Haider, M.A. Identifying the origin of the limiting process in a double perovskite PrBa_{0.5}Sr_{0.5}Co_{1.5}Fe_{0.5}O_{5+δ} thin-film electrode for solid oxide fuel cells. *ACS Appl. Mater. Interfaces*, **2019**, *11*(28), 25243-25253.
<http://dx.doi.org/10.1021/acsami.9b06666> PMID: 31260249
- [111] O'hayre, R.; Cha, S-W.; Colella, W.; Prinz, F.B. *Fuel cell fundamentals*; John Wiley & Sons, **2016**.
<http://dx.doi.org/10.1002/9781119191766>
- [112] Oladosu, T.L.; Baheta, A.T.; Hussain, P. Liquid desiccant membrane regeneration of des for air conditioning systems using electro-dialysis technique. *Advances in manufacturing engineering*; Springer, **2020**, pp. 243-252.
- [113] La Cerva, M.; Gurreri, L.; Tedesco, M.; Cipollina, A.; Ciofalo, M.; Tamburini, A. Determination of limiting current density and current efficiency in electro-dialysis units. *Desalination*, **2018**, *445*, 138-148.
<http://dx.doi.org/10.1016/j.desal.2018.07.028>
- [114] Du, D-j.; Pu, W-f.; Zhang, S.; Jin, F-y.; Wang, S-k.; Ren, F. Preparation and migration study of graphene oxide-grafted polymeric microspheres: EOR implications. *J. Petrol. Sci. Eng.*, **2020**, 107286.
<http://dx.doi.org/10.1016/j.petrol.2020.107286>
- [115] Sikiru, S.; Yahya, N.; Soleimani, H.; Ali, A.M.; Afeez, Y. Impact of ionic-electromagnetic field interaction on Maxwell-Wagner polarization in porous medium. *J. Mol. Liq.*, **2020**, *318*, 114039.
<http://dx.doi.org/10.1016/j.molliq.2020.114039>
- [116] Sikiru, S.; Yahya, N.; Soleimani, H. Photon-phonon interaction of surface ionic adsorption within electric double layer in reservoir sandstone. *Journal of Materials Research and Technology*, **2020**, *9*, 10957-10969.
<http://dx.doi.org/10.1016/j.jmrt.2020.07.095>
- [117] Wu, T.; Ma, Y.; Qu, Z.; Fan, J.; Li, Q.; Shi, P.; Xu, Q.; Min, Y. Black phosphorus-graphene heterostructure-supported Pd nanoparticles with superior activity and stability for ethanol electro-oxidation. *ACS Appl. Mater. Interfaces*, **2019**, *11*(5), 5136-5145.
<http://dx.doi.org/10.1021/acsami.8b20240> PMID: 30648393

Author Proofs
For Personal Use Only